Proceedings of FEDSM2000
2000 ASME Fluids Engineering Summer Meeting
June 11-15, 2000, Boston, Massachusetts, USA

FEDSM2000-11249

PARTICLE TRACKING AND EROSION PREDICTION IN THREE-DIMENSIONAL BENDS

Anthony Keating*
Srdjan Nešić
Department of Mechanical Engineering,
The University of Queensland,
Brisbane, Queensland, 4065
Australia
Email: keating@mech.uq.edu.au, srdjan@mech.uq.edu.au

ABSTRACT

Through a combination of computational fluid dynamics (CFD) and Lagrangian particle tracking, predictions of particle movement through complex geometry can be achieved. This work involves the development of a Lagrangian particle tracking algorithm, coupled with an eddy interaction model and erosion model, and it's use in the prediction of particle motion and erosion rates in three-dimensional bends.

The commercial CFD code, PHOENICS has been used to predict turbulent flow fields using the k-ε two-equation model of turbulence. These have been verified against known experimental results. Using a stochastic procedure, solid particles are tracked through the domain in a Lagrangian manner using the Lagrangian equation of motion of a particle. From this particle motion, impacts with solid boundaries are converted into erosion rates using a quantitative model of erosion. Sample particle trajectories are shown, and a description of the effect of secondary velocity on particle motion is given. The effect of particle inertia and bend orientation has been investigated. Finally, predictions of erosion rate on the walls of a three-dimensional square-sectioned U-bend are presented.

INTRODUCTION

As part of a larger project (Keating, 1999; Keating and Nešić, 2000) involving the numerical prediction of two-phase erosion-corrosion in bends, particle motion and the resulting erosion rates have been predicted using numerical tools. An approach involving the solution of the continuous (liquid) phase using Eulerian computational fluid dynamics and the discrete (particulate) phase using Lagrangian particle tracking has been used. While other techniques may be appropriate, this "Eulerian-Lagrangian" approach has been used previously by a number of researchers (Nešić and Postlethwaite, 1991; Frank and Schulze, 1994), and has been shown to be effective in similar situations. This technique is especially effective when dealing with low volumes of particles (compared to the volume of the fluid).

Single phase flow through bends has been investigated in the past, both experimentally and numerically. Chang et. al. (1983) reported both experimental and numerical results for flow through a square-sectioned U-bend. It is this work with which we compare our single phase numerical predictions presented in the present paper. Little work has been carried out for two-phase flow through bends, Wang et. al. (1996) coupled Eulerian CFD with a Lagrangian particle tracking method to predict erosion in 90° bends. However the particle tracking method used by Wang et. al. (1996) failed to account for the effect of turbulence of particle motion.

NUMERICAL MODEL

The numerical model presented here is broken down into three components: the fluid flow model, the particle tracking

*Address all correspondence to this author.

model and the erosion model. Each of these will be discussed separately.

Fluid flow modeling

Computational fluid dynamics (CFD) involves the solution of the Navier-Stokes and continuity equations. These equations are well known and are not repeated here. Full numerical solution of these equations is currently out of the reach of even the fastest supercomputers available, and as such researchers in the past have used the Reynolds-averaged Navier-Stokes (RANS) equations. The RANS equations require the approximation of the turbulent flux term. In the present work this is achieved using an isotropic eddy-viscosity assumption coupled with the standard two-equation k-ε model of turbulence. These approximations do not hold close to solid boundaries, and as such a wall approximation must be used. The standard wall function approximation has been used in the present work. Again, these equations are well known and not repeated here. For an overview of the equations used for fluid flow modeling, the reader is directed to Ferziger and Perić (1997).

Particle motion modeling

The motion of particles through the continuous phase is modeled in this work using Lagrangian particle tracking. While Eulerian modeling of this discrete phase is also possible, it is difficult to obtain particle-wall interactions, and the resulting erosion rates (Nešić, 1991). A Lagrangian description of the dispersed phase is based on the Lagrangian equation of particle motion, for example that given by Maxey (1993).

In many particulate flows, the ratio of fluid density to particle density is of the order of 10^{-3} and as such a number of terms in the general Lagrangian equation of particle motion can be ignored leaving only viscous drag and gravity. Historically the resulting equation has been solved using a method such as Runge-Kutta, however Durst et. al. (1984) linearized and solved the equation analytically for short time intervals:

$$u_p^{n+1} = u_f - (u_f - u_p^n)\exp\left(-\frac{\Delta t}{\tau_p}\right) + g\tau_p\left[1 - \exp\left(-\frac{\Delta t}{\tau_p}\right)\right] \quad (1)$$

where u_p is the particle's velocity, u_f the surrounding fluid's velocity, Δt the timestep, g gravitational acceleration and τ_p the particle relaxation time. Durst et. al. (1984) define the particle relaxation time as:

$$\tau_p = \frac{m_p}{3\pi\mu f_p d_p} \quad (2)$$

Therefore, once the continuous phase's instantaneous velocity field has been calculated, it is possible to track a particle through the domain. However one problem now remains: how to obtain the instantaneous velocity field from the solution of the RANS flow equations (which is a time-averaged velocity field with the turbulent fluctuations filtered out). The RANS solution provides two averaged turbulence quantities, turbulent kinetic energy, k, and the dissipation of turbulence, ε. An eddy interaction model (EIM) can be used to "reconstruct" the instantaneous velocity field from these two quantities and the time-averaged velocity field. Here, a particle is assumed to be in continuous interaction with a number of fluid eddies as it passes through the flow field. Each of these eddies has a finite size, the "eddy length", a finite life time, the "eddy lifetime" and an instantaneous internal velocity. It is these characteristics that must be obtained from the two turbulence quantities.

The instantaneous velocity inside an eddy is calculated from the root-mean-square value of fluctuation velocity, which is known from the value of turbulent kinetic energy:

$$k = \frac{1}{2}\left(u'_{f(rms)}{}^2 + v'_{f(rms)}{}^2 + w'_{f(rms)}{}^2\right) \quad (3)$$

and by the assumption of isotropic turbulence:

$$u'_{f(rms)} = v'_{f(rms)} = w'_{f(rms)} \quad (4)$$

If the fluid velocity fluctuations are Gaussian (and they are often), they can be approximated by using random numbers taken from a Gaussian distribution with a standard deviation equation to the root-mean-square value. Each of these fluctuations are calculated using separate random numbers, resulting in a anisotropic instantaneous velocity field.

It is the largest eddies that contribute most strongly to the dispersion of particles, and as such small eddies are ignored. These large eddies have a length equal to the Lagrangian length scale of turbulence, L_E, and a lifetime equal to the Lagrangian integral time scale, T_E. Different estimates for these properties have been proposed in literature, and no definitive answer currently exists. Milojević (1990) summarized a number of eddy lifetime expressions into a single expression using C_T, the Lagrangian integral time scale coefficient, yielding the following equation:

$$T_E = C_T\frac{k}{\varepsilon} \quad (5)$$

The Lagrangian length scale could then be expressed as:

$$L_E = T_E\sqrt{\frac{2}{3}k} \quad (6)$$

Using these, Milojević (1990) calculated different values for C_T for the most commonly used eddy property models:

$$C_T = 0.37 \quad \text{Gosman and Ioannides, 1983} \tag{7}$$

$$C_T = 0.2 \quad \text{Shuen, Chen and Faeth, 1983} \tag{8}$$

Milojević (1990) himself proposed C_T to be equal to 0.3 after computer optimization using his Lagrangian stochastic-deterministic model to predict dispersion of corn pollen particles in grid generated turbulence. It is this value of C_T that has been used in the present work.

While an EIM model is primarily based on the properties of the eddies, a number of other factors need to be considered. These include eddy creation, the crossing trajectories effect and non-homogeneous turbulence. The Lagrangian stochastic-deterministic (LSD) model proposed by Milojević (1990) accounts for these three factors. The model, as well as being extensively verified by Milojević (1990), has been used in the successful prediction of two-phase flow in a number of situations (Nešić and Postlethwaite, 1991; Frank and Schulze, 1994).

The computational time step required has been suggested by Milojević (1990) as:

$$\Delta t = 0.1 \min\left(\tau_p, \frac{\Delta x_{\text{cell}}}{u_p}, T_L, \tau_t\right) \tag{9}$$

where Δx_{cell} is the smallest distance across the computational cell, and τ_t is the estimated time for the particle to cross an eddy:

$$\tau_t = \frac{L_E}{|u_f - u_p|} \tag{10}$$

In order to transfer the fluid flow information from the Eulerian-based continuous to the Lagrangian framework used to track the particles a simple method is used. As a particle moves through the field, it's position on the Eulerian computational grid is found. Once this position is found the surrounding fluid properties can be interpolated from those calculated in the Eulerian stage of the computation.

Only one-way fluid to particle coupling has been accounted for in the current work. While two-way particle to fluid and fluid to particle coupling is possible in this framework using extra source terms in the Eulerian fluid flow equations, this was not done due to the low volumes of particles simulated.

Erosion modeling

Erosion, as defined by Finnie (1995) is "wear which occurs when solid particles entrained in a fluid stream strike a surface." No definitive theory of erosion currently exists, however a number of qualitative and quantitative models do. Only quantitative models will be discussed here. A number of erosion mechanisms have been proposed by researchers. The two most common are the *cutting* mechanism proposed by Finnie (1958) and the *wear and deformation* mechanism proposed by Bitter (1963). While Bitter's erosion model is commonly thought to be a better model in most situations, it's use is restricted due to the number of empirical constants required. As such we will only concern ourselves with Finnie's original model, and a modification to that model by Nešić (1991).

In the mid 1950s, after performing experimental studies of erosion using an erosion tester, Finnie (1958) attempted to explain the shape of the erosion curve by solving the equations of motion for a rigid particle striking a flat ductile surface. The resulting prediction for erosion of a volume, Q, removed by a particle of mass, m_p, impacting with a velocity, v_p, at an impact angle, α, was:

$$Q = C\frac{m_p v_p^2}{4p} f(\alpha) \tag{11}$$

where C is an arbitrary constant, denoting the number of particles that cut in an idealized manner, and p is the flow stress, similar to that measured in a compression or tension test. From experimental observation, Gane and Murry (1979) determined that a reasonable value for C was approximately 0.5.

In order to explain the shape of the erosion curve, Finnie et. al. (1992) proposed two "mechanisms" for different impact angles. At low impact angles ($\alpha \leq 18.5°$) particles were seen to strike the surface, removing a piece of the surface in a fashion similar to metal cutting. At impact angles beyond the point of maximum erosion ($\alpha > 18.5°$), particles come to rest on the surface and leave material piled up at the edge of each impact crater. This led Finnie to propose $f(\alpha)$ to be given as:

$$f(\alpha) = \begin{cases} (\sin 2\alpha - 3\sin^2\alpha) & \text{for } \alpha \leq 18.5° \\ \frac{1}{3}\cos^2\alpha & \text{for } \alpha > 18.5° \end{cases} \tag{12}$$

Finnie's original model was found by Nešić (1991) to overpredict erosion downstream of a sudden expansion. Nešić, using some ideas of Bergevin (1984), proposed combining the physical reality of Bitter's model with the simplicity of Finnie's using the assumption of a critical velocity for plastic deformation. Finnie's equations were then modified using this critical velocity in place of the impact velocity:

for $\alpha \leq 18.5°$

$$Q = \frac{m_p(v_p \sin\alpha - v_{cr})}{2p}\left[v_p \cos\alpha - \frac{3}{2}(v_p \sin\alpha - v_{cr})\right] \tag{13}$$

for $\alpha > 18.5°$

$$Q = \frac{m_p(v_p \sin\alpha - v_{cr})^2}{12p} \frac{\cos^2\alpha}{\sin^2\alpha} \quad (14)$$

The critical velocities for a number of metals were empirically determined by Bitter (1963). For steel, the critical velocity, v_{sc}, was found to be equal to 0.668m/s. This value for v_{sc} along with Bergevin and Nešić's model of erosion was used by Nešić and Postlethwaite (1991) to accurately predict erosion of stainless steel by sand particles in a sudden expansion.

IMPLEMENTATION

The commercial CFD code, PHOENICS has been used for the Eulerian modeling of the continuous phase. However, due to the lack of commercially available tools, a separate Lagrangian particle tracking code was developed. This code is loosely coupled to PHOENICS, allowing for future development with different Eulerian CFD codes. The Lagrangian code is written in C++ and is highly portable.

VERIFICATION

PHOENICS, being a commercially supported product has been extensively verified by other researchers. The developed Lagrangian particle tracking code has been verified using the Snyder and Lumley particle dispersion data and is available elsewhere (Keating, 1999).

In order to ascertain the validity of the model presented in this paper, two-phase flow through a sudden axi-symmetric expansion was modeled. Here the model was found of perform well, predicting velocities of both solid and liquid phase to a good degree of accuracy, and erosion rates to a fair degree of accuracy. Details of this verification are presented elsewhere (Keating, 1999).

RESULTS

Presented in this section are the numerical predictions of two-phase flow through a square-sectioned U-bend. The results have been split into three distinct sections: fluid flow, particle motion and erosion.

Fluid flow

A detailed experimental data of turbulent flow through a square-sectioned U-bend has been carried out by Chang et. al. (1983). Figure 1 presents the geometric layout of the bend, as well as definitions of the walls used in the following discussion. Full details of the single-phase flow results and comparison with the experimental data is given in Keating (1999). Overall, a relatively good agreement with the experimental data was reached. However in a number of places, secondary velocity (velocity towards the outer or inner walls) was under-predicted. This was attributed to the failure of the isotropic turbulence model.

Figure 2 shows vector plots of secondary velocity at various measuring planes through the bend. These plots indicate the initial formation of two counter rotating vortices at the inlet plane of the bend. These vortices are driven by the pressure difference between the inner and outer walls. At the bend entrance, the two vortices fully occupy their respective half of the cross-sectional plane. As the flow moves through the bend, these vortices shrink towards the side walls. At the exit to the bend, each vortex has been stretched and there may be up to four vortices in the duct. It is these vortices which have the largest effect on particle motion in the duct.

Particle motion

Particle tracking simulations have been carried out for sand ($\rho_p = 2700$ kg/m^2, $d_p = 430$ μm) and copper ($\rho_p = 8900$ kg/m^2, $d_p = 430$ μm) particles in both a downward- and upward-facing square-sectioned U-bend. Simulations were performed at a single Reynolds number, $Re = 5.67 \times 10^4$ with a particle concentration of 2% (volume ratio).

Sand particle trajectories for both a downward- and upward-facing U-bend are given in Figure 3. Two lines of starting locations were used at different depths in the duct (x/D = 0.2 and x/D = 0.4). Ten starting locations are located along each of these lines with one particle trajectory shown for each starting location.

Clearly, the effect of bend orientation is a large one. This is due to the effect of gravity on the particle motion. Two orientations were investigated. The first is when particles enter the bend away from the ground, then leave towards to the ground (denoted here as a *downward-facing* bend). The other orientation is when particles enter the bend towards the ground, then leave away from the ground (denoted here as a *upward-facing* bend).

Particle motion in the three-dimensional square-sectioned U-bend is extremely complex and amounts to a balance of three forces: gravity, particle inertia and the fluid's primary and secondary motion. In a downward-facing bend, particles that enter the bend near the plane of symmetry move towards the corner of the outer and side walls. The motion of particles towards the outer wall due to their inertia, counteracts the force of gravity. As neither particle inertia nor gravity has any (significant) force in the vertical plane (i.e. towards the side walls), particles are easily moved by the secondary motion towards the side walls. Particles which enter the bend near the side walls also move towards the corner of the outer and side walls, primarily by their own inertia. By the time particles reach the latter half of the bend, a large amount of their inertia has been lost. Gravity and the secondary motion now pull particles towards the inner wall.

In the upward-facing bend, particles impact the outer wall at a point closer to the inlet plane due to gravity acting with particle inertia rather than against it. The secondary velocity in the vertical plane still moves particles towards the side walls. Particles rarely impact the inner wall as gravity no longer acts in that direction.

Figure 4 shows copper particle trajectories for a downward- and upward-facing U-bend. The differences between these results and those for the sand particles are due both the increased inertia of the particle and the increased gravity force (due to their higher density). In the downward-facing bend, an increase in impacts on the inner wall is seen with the copper particles. This is due to the increased gravity force. Particles also impact, due to their increased inertia, the outer wall at a point closer to the inlet plane. As copper particles have an increased inertia and gravity force, particle trajectories in the upward-facing bend show a larger concentration of particle near the outer wall than the sand particles.

Erosion

Averaged erosion rates have been obtained through the stochastic averaging of 16000 particle trajectories, released from a rectangular array in the inlet of the bend. Due to the normal impact velocity always being less than the critical value proposed by Bitter (1963), the modified erosion model failed to predict erosion. Therefore all the erosion rates presented here were obtained using Finnie's original erosion model.

For sand particles, predictions at five measuring planes (0°, 45°, 90°, 135°, 180° and downstream of the bend) are shown in Figure 5 (downward-facing) and Figure 6 (upward-facing). Peak values of erosion are summarized in Table 1.

In the case of an downward-facing bend, peak values of erosion caused by sand particles occur at the corner of the outer and side walls near the exit plane (180° in the bend). These occur due to particle inertia causing particles to move towards the outer wall, and the secondary motion in the duct causing movement towards the side walls (see discussion in the previous section).

A much smaller peak in erosion rate is seen at 90° in the bend at the centerline of the outer wall. This is the position where particles start moving towards the side walls. In some instances the secondary velocity turns the particle before it impacts with the outer wall, in other instances a particle may impact the outer wall and cause erosive damage. A diagonal erosion "line" from this point to the corner of the side and outer walls at 180° can be seen in the results.

Some impacts do occur on the inner wall, and as such a second peak in erosion can be seen near the corner of the inner and side walls.

In an upward-facing bend, particles impact the outer wall at a point closer to the inlet plane (maximum erosion at 131°). Erosion rates in the upward-facing bend are higher than those predicted for the downward-facing bend due to gravity adding to particle inertia rather than subtracting from. Particles also impact at the centerline of the outer wall due the same effect discussed for the downward-facing bend. However this impact point is closer to the inlet plane (due to gravity and particle inertia being pointed in the same direction).

	downward	upward
Inner wall		
Erosion rate (mm/yr)	35.52	
Position in bend	49°	
x (distance from centerline)	0.0205	
Outer wall		
Erosion rate (mm/yr)	180.19	3055.76
Position in bend	180°	131°
x (distance from centerline)	0.0217	0.0217
Side walls		
Erosion rate (mm/yr)	161.22	2733.99
Position in bend	180°	131°
y (distance from inner wall)	0.0440	0.0440

Table 1. PREDICTIONS OF PEAK EROSION RATE AND THE POSITION OF THE PEAK FOR SAND PARTICLES.

Due to the lack of impacts on the inner wall (the reason for which has been discussed previously), no erosion was predicted to occur on the inner wall for the upward-facing bend. Erosion on the side walls matched that on the outer wall in both cases.

For copper particles, erosion curves are similar to those predicted for the sand particles, however the magnitude of erosion rates have increased. Table 2 shows peak erosion rates for copper particles. Compared to the peak erosion rates for sand particles, only two differences (other than the magnitude of erosion rate) can be seen. The first is the position of the peak in erosion rate on the inner wall which has moved closer to the outlet plane. The second difference is in the position of the peak in erosion on the outer and side walls for the upward-facing bend. This peak has moved towards the inlet plane of the bend, due to the increase in particle inertia.

CONCLUSIONS

1. A Lagrangian particle tracking and erosion prediction code has been developed and linked with a Eulerian computational fluid dynamics (CFD) package. The code implements

	downward	upward
Inner wall		
Erosion rate (mm/yr)	234.5	
Position in bend	109°	
x (distance from centerline)	0.0217	
Outer wall		
Erosion rate (mm/yr)	2039.2	19229.6
Position in bend	180°	124°
x (distance from centerline)	0.0217	0.0217
Side walls		
Erosion rate (mm/yr)	1824.45	17204.9
Position in bend	180°	124°
y (distance from inner wall)	0.0440	0.044

Table 2. PREDICTIONS OF PEAK EROSION RATE AND THE POSITION OF THE PEAK FOR COPPER PARTICLES.

the Lagrangian description of particle motion, coupled with an eddy-interaction model and fully accounts for the effect of turbulence on particle motion. Two erosion models, Finnie's and a modification of Finnie's are included.

2. Predictions of particle motion in a three-dimensional square-sectioned U-bend have been presented. Here is was found that the fluid's secondary motion in the bend had a significant effect on particle motion. The orientation of the bend (in which direction gravity acted) was also found to have a large effect on particle motion.
3. Using wall-interaction data collected from averaged particle motion and a quantitative erosion model, erosion rates were calculated. Maximum erosion rates occurred in the corner of the outer and side walls of the bend for both orientations. As expected, erosion rates in the upwards-facing bend were much greater than for the downwards facing bend.
4. The modified erosion model proposed by Nešić failed to predict erosion to occur for this particular situation. This was due to the normal impact velocity of the particles to be less than the critical value for plastic deformation suggested by Bitter.
5. It is important to note that the numerical predictions given here have not been compared to experimental data. This was due to the lack of detailed experimental data for localized erosion in bends. It is essential that before further numerical work is carried out, that a number of experiments are performed which provide detailed information on particle motion and erosion in similar geometries.

REFERENCES

Bergevin, K., *Effect of slurry velocity on the mechanical end electrochemical components of erosion-corrosion in vertical pipes*, Masthers thesis, University of Saskatchewan, Saskatoon, Canada, 1984.

Bitter, J. P. A., *A study of erosion phenomena, Part I*, Wear, Vol. 6, 1963.

Bitter, J. P. A., *A study of erosion phenomena, Part 2*, Wear, Vol. 6, 1963.

Chang, S. M., Humphrey, J. A. C., and Modavi, A., *Turbulent flow in a strongly curved U-bend and downstream tangent of square cross-sections*, PhysicoChemical Hydrodynamics, Vol. 4, Number 3, pp. 243–269, 1983.

Durst, F., Milojević, D., and Schönung, B., *Eulerian and Lagrangian predictions of particle two-phase flows: A numerical study*, Applied Mathematical Modeling, Vol. 8, pp. 101–115, 1984.

Ferziger, J. H. and Perić, M., *Computational Methods for Fluid Dynamics*, Springer-Verlag, Belin, 1997.

Finnie, I., *The mechanism of erosion of ductile materials*, In proceedings 3rd US Natl. Congress of Applied Mechanics, pp. 527–532, 1958.

Finnie, I., *Some reflections on the past and future of erosion*, Wear, Vol. 186–187, pp. 1–10, 1995.

Finnie, I., Stevick, G. R., and Ridgeley, J. R., *The influence of impingement angle on the erosion of ductile metals by angular abrasive particles*, Wear, Vol. 152, pp. 91–98, 1992.

Frank, T. and Schulze, I., *Numerical simulation of gas-droplet flow around a nozzle in a cylindrical chamber using a Lagrangrian model based on a multigrid Navier-Stokes solver*, In proceedings Int. Symposium on Numerical Methods for Multiphase Flows, ASME Fluids Engineering Division, Summer Meeting, June 19–23, Lake Tahoe, Nevada, U.S.A., 1994.

Gane, N. and Murry, M. J., *The transition from ploughing to cutting in erosive wear*, In proceedings 5th International Conference on Erosion by Solid and Liquid Impact, Cambridge, U.K., 1979.

Gosman, A. D., and Ioannides, E., *Aspects of computer simulation of liquid-fuelled combustors*, Journal of Energy, Vol. 7, pp. 482–490, 1983.

Keating, A., *A model for the investigation of two-phase erosion-corrosion in complex geometries*, Masters thesis, The University of Queensland, Queensland, Australia, 1999

Keating, A. and Nešić S., *Numerical prediction of erosion-corrosion in bends*, In proceedings NACE Corrosion 2000, March 26–31, Orlando, Florida, U.S.A., 2000

Maxey, M. R., *The equation of motion for a small rigid*

sphere in a nonuniform or unsteady flow, ASME/FED Gas-Solid Flows, Vol. 166, pp. 57–62, 1993.

Milojević, D., *Lagrangian stochastic-determinstic (LSD) predictions of particle dispersion in turbulence*, Part. Part. Sys. Charact., Vol. 7, pp. 181–190, 1990.

Nešić, S., *Computation of localized erosion-corrosion in disturbed two-phase flow*, PhD thesis, University of Saskatchewan, Saskatoon, Canada, 1991.

Nešić, S. and Postlethwaite, J., *Hydrodynamics of disturbed flow and erosion-corrosion, Part II. Two-phase flow study*, The Canadian Journal of Chemical Engineering, Vol. 69, pp. 704–710, June 1991.

Shuen, J. S., Chen, L. D., and Faeth, G. M., *Evaluation of a stochastic model of particle dispersion in a turbulent round jet*, AIChE Journal, Vol. 29, No. 1, pp. 167–170, 1983.

Snyder, W. H. and Lumley, J. L., *Some measurements of particle velocity autocorrelation functions in turbulent flow*, Journal of Fluid Mechanics, Vol. 48, pp. 41–71, 1971.

Wang, J., Shirazi, S. A., Shadley, J. R., and Rybicki, E. F., *Application of flow modeling and particle tracking to predict sand erosion rates in 90 degree elbows*, In FED Vol. 236, 1996 Fluids Engineering Division Conference, Vol. 1, pp. 725–734, 1996.

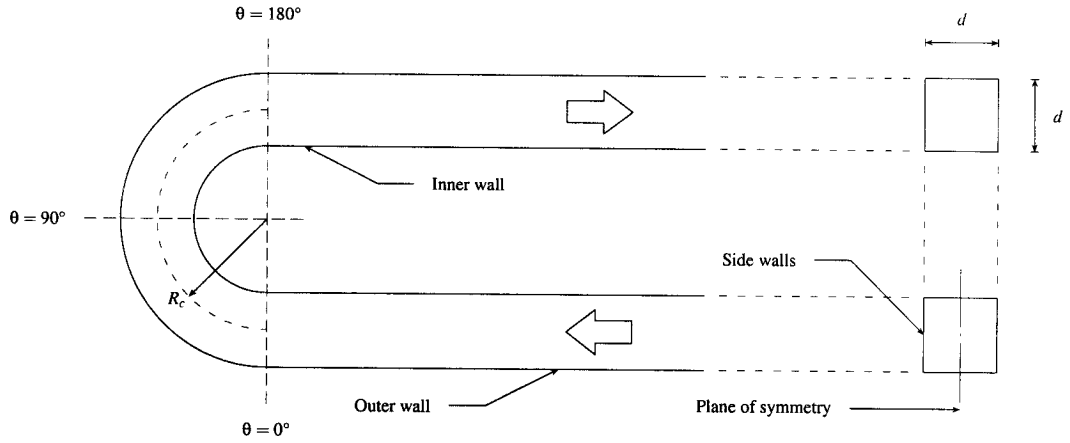

Figure 1. GEOMETRIC LAYOUT OF THE THREE-DIMENSIONAL SQUARE-SECTIONED U-BEND, INCLUDING DEFINITIONS OF INNER, OUTER AND SIDE WALLS.

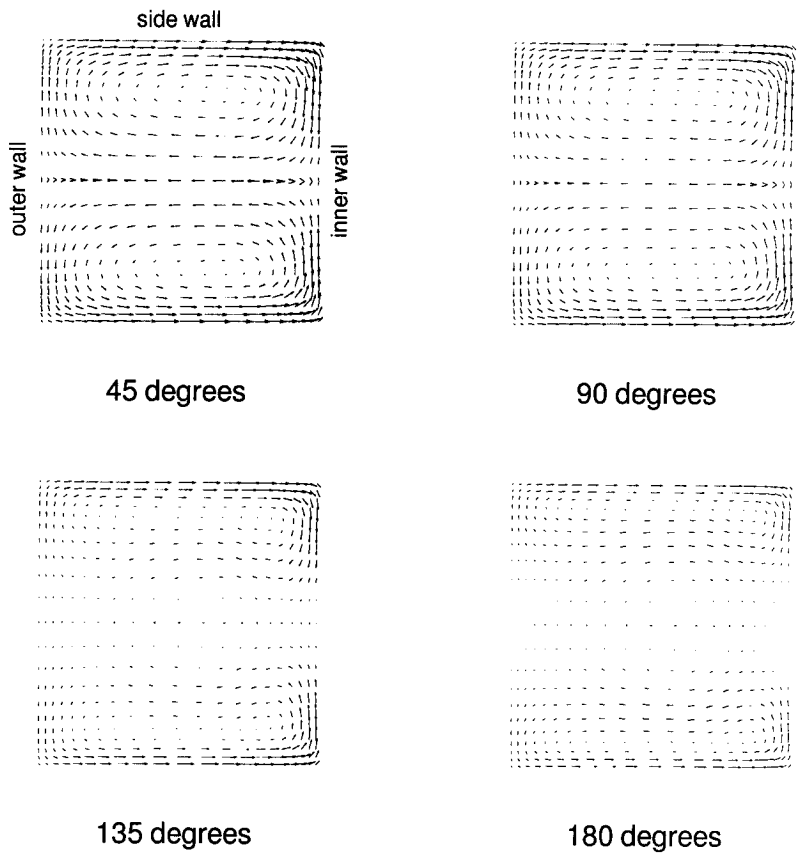

Figure 2. PREDICTIONS OF SECONDARY MOTION AT FOUR PLANES IN THE BEND.

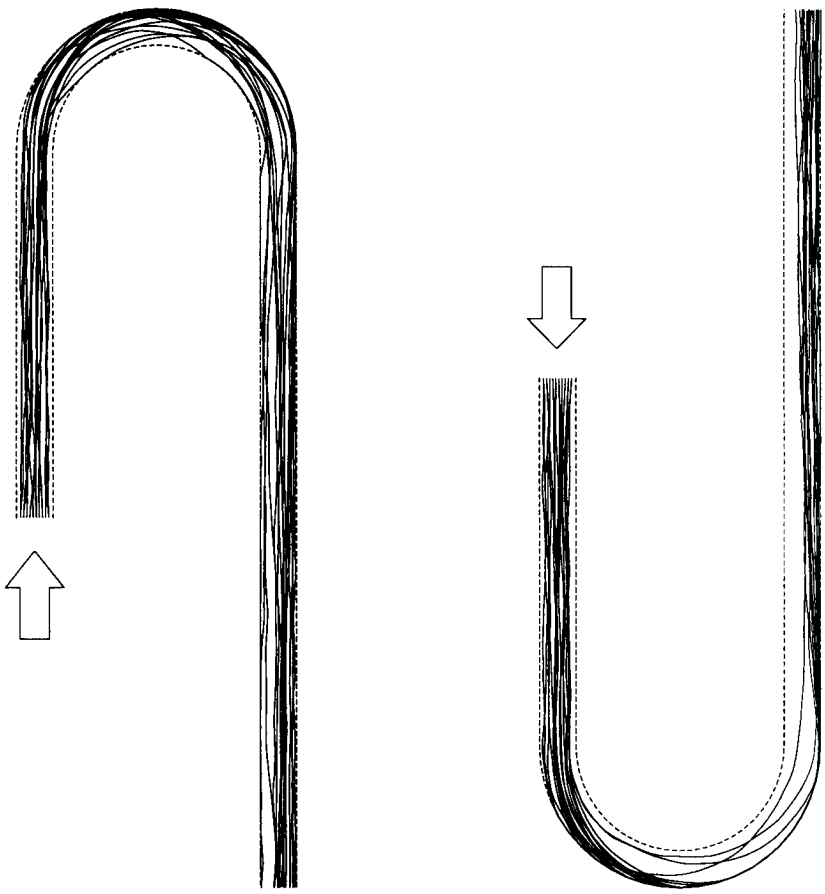

Figure 3. SAMPLE PARTICLE TRAJECTORIES FOR SAND PARTICLES.

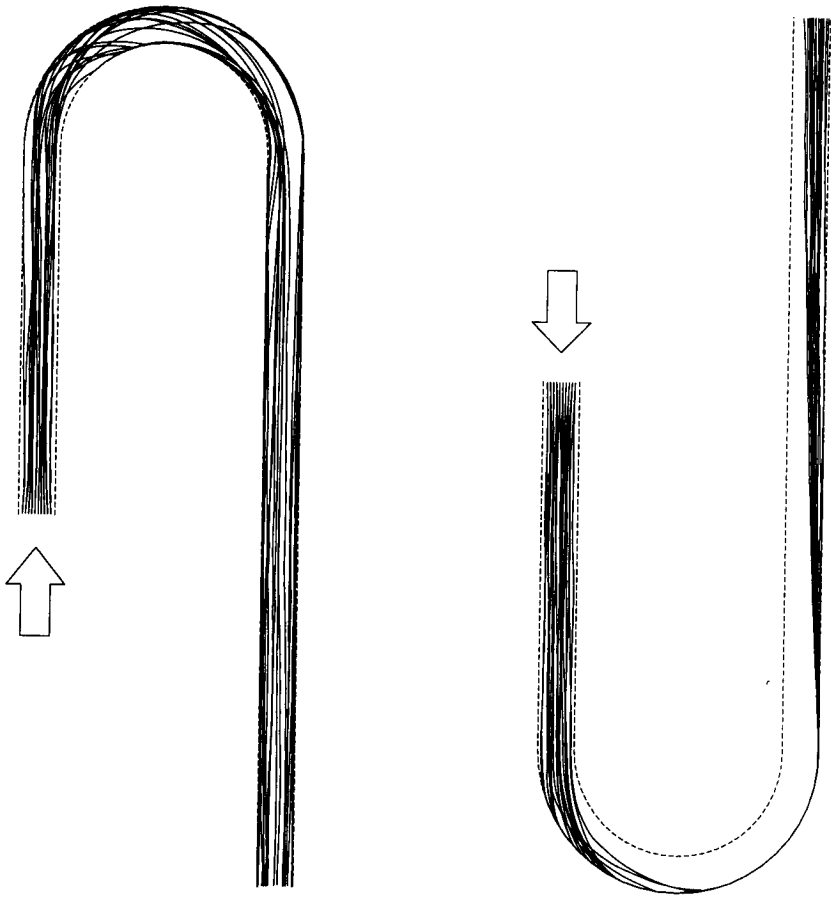

Figure 4. SAMPLE PARTICLE TRAJECTORIES FOR COPPER PARTICLES.

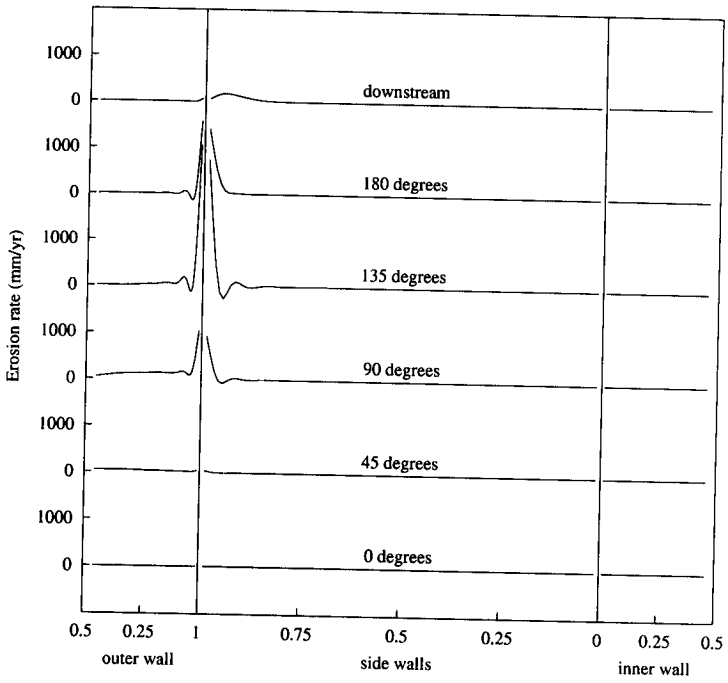

Figure 5. PREDICTED EROSION RATE FOR SAND PARTICLES ON THE OUTER, SIDE AND INNER WALLS OF AN UPWARDS-FACING BEND. AVERAGED OVER 16000 TRAJECTORIES.

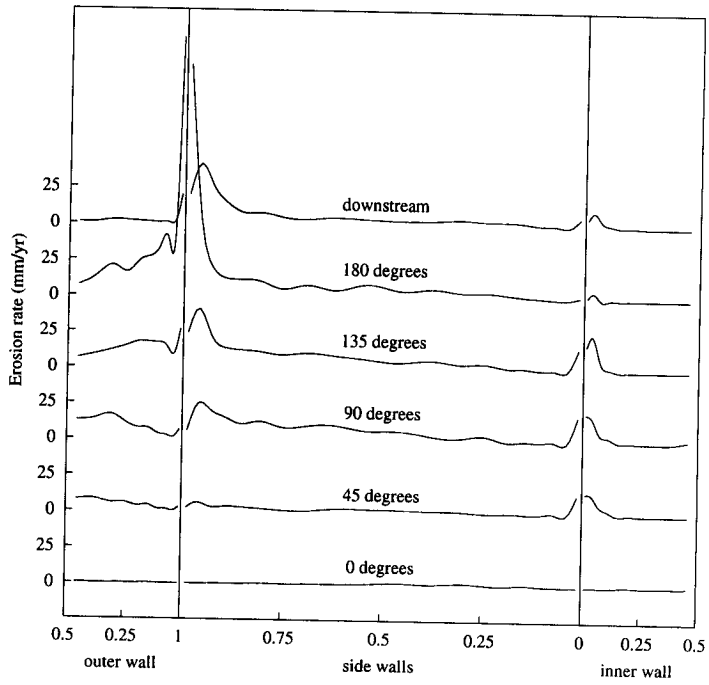

Figure 6. PREDICTED EROSION RATE FOR SAND PARTICLES ON THE OUTER, SIDE AND INNER WALLS OF A DOWNWARDS-FACING BEND. AVERAGED OVER 16000 TRAJECTORIES.